Electronic Magnetization of a Quantum Point Contact Measured by Nuclear Magnetic Resonance

Minoru Kawamura,[1,*] Keiji Ono,[1] Peter Stano,[1,2] Kimitoshi Kono,[1] and Tomosuke Aono[3]
[1]RIKEN Center for Emergent Matter Science, Wako 351-0198, Japan
[2]Institute of Physics, Slovak Academy of Sciences, 84511 Bratislava, Slovakia
[3]Department of Electrical and Electronic Engineering, Ibaraki University, Hitachi 316-8511, Japan
(Received 23 February 2015; published 13 July 2015)

We report an electronic magnetization measurement of a quantum point contact (QPC) based on nuclear magnetic resonance (NMR) spectroscopy. We find that NMR signals can be detected by measuring the QPC conductance under in-plane magnetic fields. This makes it possible to measure, from Knight shifts of the NMR spectra, the electronic magnetization of a QPC containing only a few electron spins. The magnetization changes smoothly with the QPC potential barrier height and peaks at the conductance plateau of $0.5 \times 2e^2/h$. The observed features are well captured by a model calculation assuming a smooth potential barrier, supporting a no bound state origin of the 0.7 structure.

DOI: 10.1103/PhysRevLett.115.036601 PACS numbers: 72.25.Dc, 72.25.Pn, 73.23.Ad, 76.70.Fz

Quantum point contact (QPC) is a short one-dimensional (1D) channel connecting two electron reservoirs. Its conductance is quantized to integer multiples of $2e^2/h$, where e is electron charge and h is Planck's constant [1,2]. The conductance quantization is well understood within a model of noninteracting electrons [3]. However, experiments have shown an additional conductance feature, a shoulderlike structure at around $0.7 \times 2e^2/h$ termed a 0.7 structure [4,5]. Despite the simplicity of a QPC, a comprehensive understanding of the 0.7 structure is still lacking [6–19].

Theories proposed to explain the 0.7 structure can be discriminated according to their predictions on the electron spin arrangement, which include spontaneous spin polarization [6,7], antiferromagnetic Wigner crystal [8], Kondo screening [9–11], and local spin fluctuations accompanied by van Hove singularity [12,13]. Especially in the Kondo scenario, the existence of a localized magnetic moment in the QPC is an inevitable ingredient. On one hand, early experiments observing Fano resonances suggested a presence of such a local single spin trapped in a bound state regardless of magnetic fields [14]. On the other hand, an experiment measuring compressibility contradicts such a bound state formation [18]. Thus, the degree of spin polarization of a QPC is one of the central issues in understanding the origin of the 0.7 structure.

However, most experiments [4,5,14–17] to date have focused on transmission properties, without the QPC spin polarization being addressed directly. Despite the recent progress in magnetic sensors [20], the magnetization measurement of a QPC containing only a few electrons is still very challenging. Recently, small magnetizations of two-dimensional electron systems (2DESs) embedded in GaAs have been measured [21–23] by combining techniques of current-induced nuclear spin polarization [24–28] and resistance (conductance) detection of nuclear magnetic resonance (NMR) signals of Ga and As nuclei [27–29]. Because of the hyperfine interaction between electronic and nuclear spins, an electronic magnetization produces an effective magnetic field for nuclei, resulting in the shift of the NMR frequency, the Knight shift. From the Knight shift, the electronic magnetization can be determined [30].

A recent transport experiment by Ren *et al.* [31] suggests such an influence of nuclear spins on the QPC conductance. They observed hysteresis in the source-drain voltage dependence of the differential conductance under magnetic fields, and they attributed its origin to the dynamical nuclear spin polarization (DNSP) induced in the QPC. However, NMR or other direct evidence showing involvement of nuclear spins has not been presented so far. NMR signal detection in the QPC conductance would constitute a novel experimental technique to probe spin properties of QPCs or nanowires [32,33].

In this Letter, we report an electronic magnetization measurement of a QPC defined in a GaAs/AlGaAs heterostructure based on NMR spectroscopy. We find that the QPC differential conductance changes when the frequency of an applied oscillating magnetic field matches the NMR frequencies of ^{69}Ga, ^{71}Ga, and ^{75}As. The resistive detection of the NMR signals allows us to measure the electronic magnetization of the QPC from the Knight shifts of the NMR spectra. The Knight shift measurements are conducted at the QPC conductance between 0 and $2e^2/h$ by tuning gate and source-drain voltages. The magnetization changes smoothly with the QPC potential barrier height and peaks at the conductance plateau of $0.5 \times 2e^2/h$. The observed features are well captured by a model calculation assuming a smooth potential barrier without a bound state being formed. Apart from the demonstration of a new technique to measure a magnetization of only a few electrons, the absence of a bound state in the QPC is

our main conclusion, directly relevant for the understanding of the 0.7 structure.

QPCs studied in this work are fabricated from a wafer of $GaAs/Al_{0.3}Ga_{0.7}As$ single heterostructure with a 2DES at the interface. The mobility and sheet carrier density of the 2DES at 4.2 K are 110 $m^2/V\,s$ and 2.2×10^{15} m^{-2}, respectively. A QPC is defined electrostatically applying negative voltages (V_{g1}, V_{g2}) to a pair of Au/Ti gate electrodes patterned on the surface of the wafer. All data presented here are measured on a QPC with lithographic dimensions of 300 nm length and 250 nm width [inset of Fig. 1(a)], in a dilution refrigerator at the mixing chamber temperature of 20 mK. The external magnetic field B is applied parallel to the 2DES plane along the current flowing direction [the x direction in the inset of Fig. 1(a)] to avoid orbital effects and quantum Hall edge channels. The differential conductance $G = dI/dV_{sd}$ (where I is the current and V_{sd} is the source-drain bias voltage) is measured using a standard lock-in technique with a typical excitation voltage of 20 μV at 118 Hz. A single-turn coil is wound around the device to apply radio-frequency oscillating magnetic field B_{rf}.

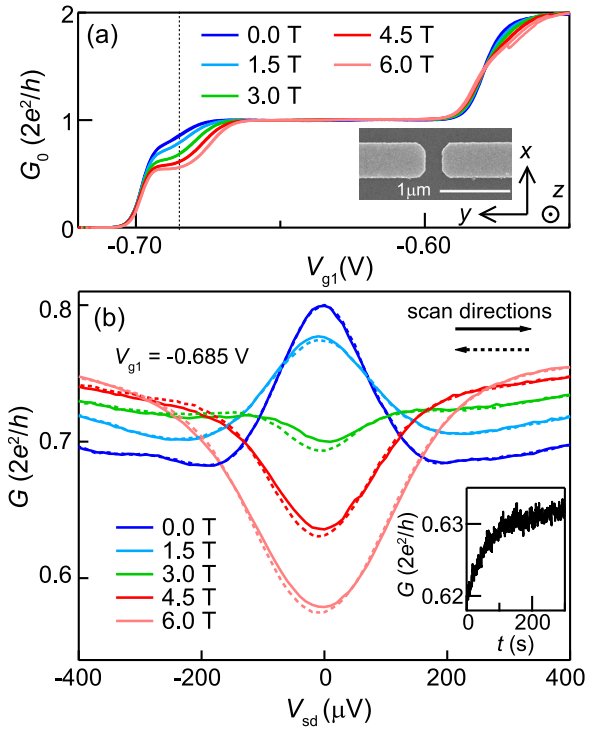

FIG. 1 (color online). (a) Linear conductance G_0 as a function of V_{g1} ($V_{g2} = -1.4$ V) at $B = 0$, 1.5, 3, 4.5, and 6 T, applied along the x direction. Inset shows a scanning electron microscope image of the device. (b) Differential conductance G as a function of source-drain bias voltage V_{sd} at $V_{g1} = -0.685$ V [indicated by a dashed line in (a)] under the same magnetic fields as in (a). The solid (dashed) curves are measured by scanning V_{sd} in the positive (negative) direction at a rate of 5.6 μV/s. The inset shows the time dependence of G at $B = 4.5$ T and $V_{g1} = -0.685$ V after an instantaneous change of V_{sd} from 0 to -50 μV. A slightly different value compared to the one in (b) for the same parameters, $B = 4.5$ T and $V_{sd} = -50$ μV, arises due to a remaining DNSP created at large $|V_{sd}|$ during the V_{sd} scan in (b).

The QPC shows a typical conductance quantization behavior. Figure 1(a) shows linear conductance $G_0 = G(V_{sd} = 0)$ as a function of gate voltage V_{g1}. In addition to quantized conductance plateaus, the 0.7 structure is observed at the zero magnetic field, developing into a plateau of $0.5 \times 2e^2/h$ at high magnetic fields. A zero-bias conductance peak accompanying the 0.7 structure is observed clearly in the $G - V_{sd}$ curve at $B = 0$ T [Fig. 1(b)]. With an increasing B, the zero-bias conductance peak is suppressed and turns into a dip above $B = 3$ T.

Hysteresis is observed in the $G - V_{sd}$ curves when V_{sd} is scanned slowly (5.6 μV/s) in the positive and negative directions [Fig. 1(b)]. The hysteresis is seen only at finite magnetic fields. The typical time scale for developing the hysteresis is measured at $B = 4.5$ T by recording G after an instantaneous change of V_{sd} from 0 to -50 μV [the inset of Fig. 1(b)]. The value of G continues to change over a period of 200 s. This time scale is consistent with nuclear spin relaxation or polarization times reported in GaAs-based devices [27,28,31,34,35]. Similarly, as concluded in an earlier work [31], we interpret the slow change in G as the first indication of DNSP in the QPC.

To confirm the nuclear spin origin of the observed slow change in G, we perform the NMR spectroscopy experiment. Scanning the frequency f of B_{rf}, we observe decreases in G when f matches the NMR frequency of ^{75}As (gyromagnetic ratio $\gamma = 45.82$ rad MHz/T) (Fig. 2). The obtained $G - f$ curve represents the NMR spectrum of ^{75}As, split into three dips due to the electric quadrupole interaction [36]. We observe signals at resonances of ^{69}Ga and ^{71}Ga, as well as analogous behavior in four other QPC devices (not shown). These observations clearly show that the DNSP is induced in the QPC and that its changes are measured by monitoring the QPC conductance.

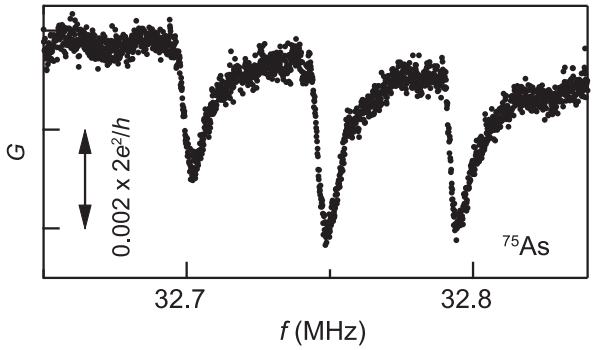

FIG. 2. Differential conductance G as a function of frequency f of B_{rf} at $B = 4.5$ T, $V_{g1} = -0.685$ V, and $V_{sd} = -50$ μV. B_{rf} is applied perpendicular to B [the y direction in the inset of Fig. 1(a)]. f is scanned at a rate of 0.128 kHz/s. Data of ten subsequent measurements are averaged to improve the signal to noise ratio.

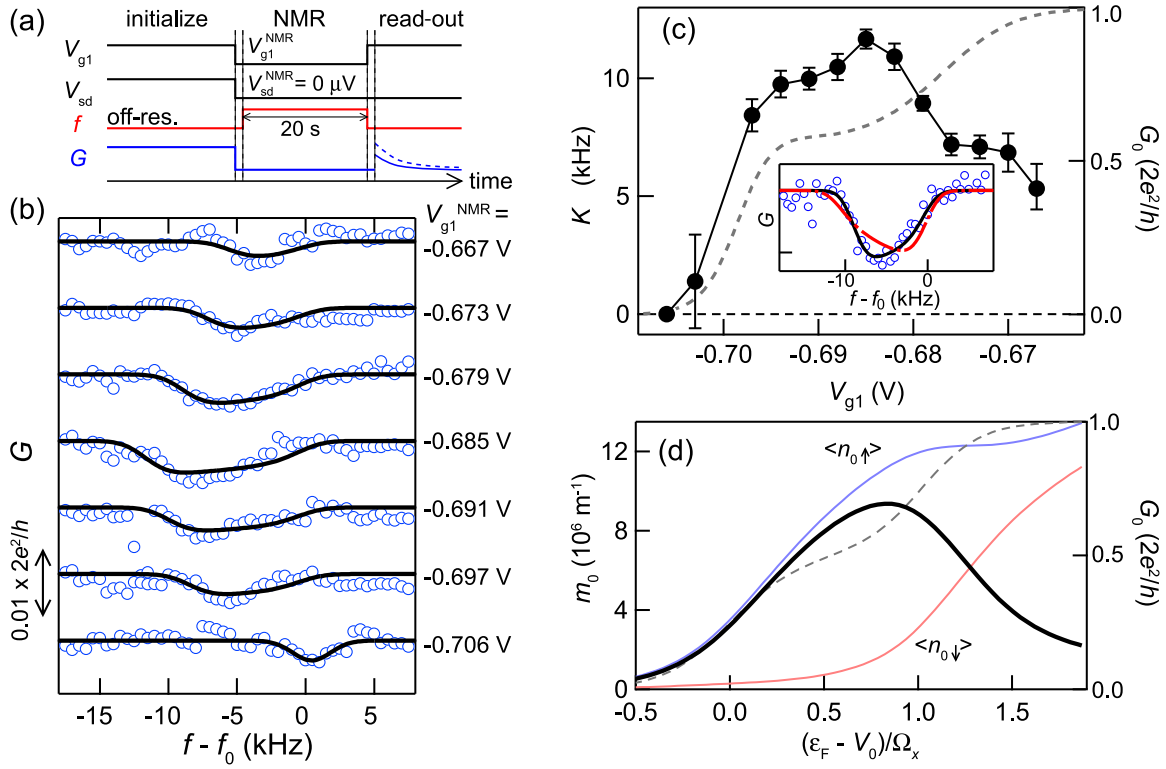

FIG. 3 (color online). (a) Schematic sequence for the pump-probe experiment. (b) NMR spectra of ^{75}As for $V_{sd}^{NMR} = 0$ μV and various gate voltages V_{g1}^{NMR}, as indicated. NMR signals corresponding to the transition between nuclear spin states $|I_z = \pm 1/2\rangle$ are shown. Solid curves are the fitting results. Data are offset vertically for clarity. (c) Knight shift K plotted as a function of gate voltage V_{g1}. Linear conductance G_0 is plotted by a dotted curve referring to the right axis. Inset shows fitting results of the NMR data for $V_{g1}^{NMR} = -0.679$ V assuming 3D (dashed) and 2D (solid) hard-wall confinement potentials. (d) Calculated magnetization density at the QPC center m_0 plotted as a function of potential barrier height V_0. The red and blue curves depict spin densities $\langle n_{0,\uparrow}\rangle$ and $\langle n_{0,\downarrow}\rangle$, respectively. Calculated conductance G_0 is plotted by a dotted curve referring to the right axis.

Having established the method to probe the NMR spectra in transport, we now use it to determine the electronic magnetization of the QPC. To this end, we perform the following pump-probe experiment [Fig. 3(a)]. First, nuclear spins are initialized by inducing DNSP under a relatively large bias voltage $V_{sd} = -300$ μV at $V_{g1} = -0.685$ V. Then, V_{sd} is set to 0 μV and the QPC is tuned to a state of interest by setting the gate voltage to V_{g1}^{NMR} for a period of time (22 s), during which the frequency of B_{rf} is set to f for 20 s [41]. Finally, changes in the DNSP are read out by recording G with a small ac voltage excitation (20 μV, 118 Hz) at $V_{g1} = -0.685$ V and $V_{sd} = 0$ μV. The observed values of G at the beginning of the read-out step reflect how much the nuclear spins are depolarized by B_{rf}. Repeating this procedure with different f, we obtain a NMR spectrum for a gate voltage V_{g1}^{NMR}, as shown in Fig. 3(b).

The bottom data of Fig. 3(b) are obtained by depleting electrons from the QPC during the B_{rf} application. Therefore, this spectrum is not affected by electrons and has a rather sharp dip at $f_0 = 32.755$ MHz, the frequency corresponding to the transition between the nuclear spin states $|I_z = \pm 1/2\rangle$. As V_{g1}^{NMR} is increased, the NMR induced dips are shifted toward negative frequencies and broadened. These shifts are the Knight shifts due to the electronic magnetizations in the QPC.

We now evaluate the magnitude of the Knight shifts by taking the spatial electron distribution into account. Extending earlier works [21,22,42], we adopt a model of electrons confined in the y and z directions with a transverse wave function $\psi(y,z)$. The Knight shift for an As nucleus at position (y,z) can be written as $\delta f_K(y,z) = \alpha_{As} m_z |\psi(y,z)|^2$, where $\alpha_{As} = -2.1 \times 10^{-22}$ kHz m^3 is the hyperfine coupling coefficient [36], and $m_z \equiv n_\uparrow - n_\downarrow$ is 1D electronic magnetization density defined as the difference in 1D spin densities. We make a standard assumption [42] that nuclear spins are depolarized by the rf-magnetic field according to the detuning from the resonance $\delta f = f - (f_0 + \delta f_K)$ with a Gaussian profile $\exp(-\delta f^2/2\gamma^2)$, where f_0 and γ are the NMR frequency and the spectrum width without the influence of the Knight shift, respectively. Such depolarizations induce the change in the electron Zeeman energy which is given by an integral of local nuclear spin depolarization multiplied by electron distribution. Since these changes are small, we may expand

the QPC conductance, which is a function of the electron Zeeman energy, and get for its change

$$\delta G(f) = A \int dydz \exp(-\delta f^2/2\gamma^2)|\psi(y,z)|^2, \quad (1)$$

with A being an unknown proportionality coefficient. To evaluate Eq. (1), we approximate the transverse wave function by the one of a two-dimensional (2D) hard-wall confinement, $\psi(y,z) \propto \cos(\pi y/w_y)\cos(\pi z/w_z)$, with confinement widths $w_y = (65 \pm 5)$ nm and $w_z = (18 \pm 3)$ nm [43]. The Knight shift becomes $\delta f_K(y,z) = -K\cos^2(\pi y/w_y)\cos^2(\pi z/w_z)$, with a parameter K proportional to m_z via $K = -\alpha_{\mathrm{As}} m_z |\psi(0,0)|^2$. The experimental data in Fig. 3(b) are fitted to Eq. (1) using K and A as fitting parameters, with $f_0 = 32.755$ MHz and $\gamma = 1.36$ kHz determined from the data measured at the depletion configuration ($V_{g1}^{\mathrm{NMR}} = -0.706$ V). As seen in the figure, the agreement of the data and the model fitted for each curve is excellent.

We now consider an alternative fit, assuming that the QPC transport occurs through a three-dimensionally (3D) confined electronic state $\psi(x,y,z) \propto \cos(\pi x/w_x)\cos(\pi y/w_y)\cos(\pi z/w_z)$. A representative result, using an analog of Eq. (1), is given in the inset of Fig. 3(c) and shows a much worse compatibility with the data. We find that such a discrepancy is not sensitive to the confinement details. As is especially well visible for large Knight shifts, the data show a skewed line shape, with steep (gentle) slopes on the low (high) frequency side. This is systematically reproduced by 2D confinement models, unlike 3D ones (see the Supplemental Material [36]).

In Fig. 3(c), K is plotted as a function of V_{g1}. A finite K emerges near the conductance onset and increases steeply as the conductance is increased to $0.5 \times 2e^2/h$. It keeps increasing gradually with an increasing V_{g1}, even in the conductance plateau region of $0.5 \times 2e^2/h$. As V_{g1} is increased further, K begins to decrease, accompanied by a rise of conductance from $0.5 \times 2e^2/h$. As a result, a peak in K is formed at the high gate-voltage end of the conductance plateau. Using the relation between K and m_z, the observed maximum value $K = (11.7 \pm 0.5)$ kHz corresponds to $m_z = (16.5 \pm 4.5) \times 10^6$ m^{-1}.

We now show that the observed features are well reproduced by a model calculation. We model a QPC by a 1D tight-binding Hamiltonian,

$$H = \sum_{j,\sigma} \epsilon_{j,\sigma} c_{j,\sigma}^\dagger c_{j,\sigma} - t \sum_{j,\sigma} c_{j,\sigma}^\dagger c_{j+1,\sigma} + \sum_j U_j n_{j,\uparrow} n_{j,\downarrow}. \quad (2)$$

Here, $c_{j,\sigma}^\dagger$ creates an electron with spin $\sigma (\sigma = \uparrow, \downarrow)$ at the jth site of the tight-binding chain which has a hopping amplitude t. We assume a short-range Coulomb interaction represented by the on-site Coulomb energy U_j. The potential energy and the Zeeman energy are included in the on-site energy, $\epsilon_{j,\uparrow/\downarrow} = \epsilon_j \pm g\mu_B B/2$, with the Bohr magneton μ_B and the electron g factor g. We assume a smooth parabolic potential barrier at the QPC center with a height V_0 and a curvature Ω_x. The interaction term is treated by a mean-field approximation neglecting spin fluctuations. Then the mean-field spin density $\langle n_{j,\sigma} \rangle$ is determined by a self-consistent Green's function method [45] where the on-site energy $\epsilon_{j,\sigma}$ is shifted by $U_j \langle n_{j,\bar{\sigma}} \rangle$ with $\bar{\sigma}$, the opposite spin to σ. We calculate the magnetization density profile $m_j = \langle n_{j,\uparrow} - n_{j,\downarrow} \rangle$ and the QPC conductance G_0. The values of U_j and Ω_x are determined from the conductance measurement data [36].

The thick solid curve in Fig. 3(d) depicts the calculated magnetization density at the QPC center $m_0 = m_{j=0}$ as a function of V_0, resembling the observed V_{g1} dependence of K in Fig. 3(c). According to the calculation, the increase in m_0 accompanied by the emergence of the conductance corresponds to the increase in the number of up-spin electrons in the QPC. The value of m_0 starts to decrease when down-spin electrons begin to populate the QPC, lifting G_0 from $0.5 \times 2e^2/h$. The gradual increase in m_0 in the $0.5 \times 2e^2/h$ plateau region is also reproduced. The maximum value of the calculated magnetization density $m_0 = 9.3 \times 10^6$ m^{-1} roughly agrees with the value determined from the Knight shift. Spin polarization $P = \langle n_{0,\uparrow} - n_{0,\downarrow} \rangle / \langle n_{0,\uparrow} + n_{0,\downarrow} \rangle$ reaches 70.0% where m_0 is maximal. Distribution of m_j has a bell-shaped profile and extends over a length of about 100 nm around the QPC center [36].

The gradual change in m_0 reflects the fact that the local density of states is continuous at the QPC center, unlike in a quantum dot. We therefore attribute the observed gradual change in K to be consistent with a QPC model without any bound states. This contradicts earlier observations claiming that a single-electron spin is trapped in a bound state formed in the QPC [14]. We estimate [36] that the observed magnitude of the magnetization density corresponds to the total magnetic moment (1.65 ± 0.45) in the QPC, exceeding the single-electron-spin magnetic moment which a bound state can support. Our measurement results of the NMR line shapes, the gradual change of K, and the magnetic moment values are consistent with a QPC model without bound states, such as Refs. [12,13], which predicts a smooth increase of the magnetization without saturation upon an increase of the magnetic field.

In summary, we find that the NMR signals can be detected by measuring the QPC conductance under in-plane magnetic fields. The resistive detection makes it possible to measure the electronic magnetization of the QPC from the Knight shifts of the NMR spectra. The electronic magnetization changes smoothly with the gate voltage and peaks at the conductance plateau of $0.5 \times 2e^2/h$. The gate-voltage dependence of the Knight shift is well explained by a model calculation assuming a smooth potential barrier, supporting a no bound state origin of the 0.7 structure.

This work was partially supported by Grant-in-Aid for Scientific Research No. 24684021 from Japan Society for the Promotion of Science (JSPS). We thank T. Machida for the valuable discussions.

*minoru@riken.jp

[1] D. A. Wharam, T. J. Thornton, R. Newbury, M. Pepper, H. Ahmed, J. E. F. Frost, D. G. Hasko, D. C. Peacock, D. A. Ritchie, and G. A. C. Jones, J. Phys. C **21**, L209 (1988).

[2] B. J. van Wees, H. van Houten, C. W. J. Beenakker, J. G. Williamson, L. P. Kouwenhoven, D. van der Marel, and C. T. Foxon, Phys. Rev. Lett. **60**, 848 (1988).

[3] M. Buttiker, Phys. Rev. B **41**, 7906 (1990).

[4] K. J. Thomas, J. T. Nicholls, M. Y. Simmons, M. Pepper, D. R. Mace, and D. A. Ritchie, Phys. Rev. Lett. **77**, 135 (1996).

[5] K. J. Thomas, J. T. Nicholls, N. J. Appleyard, M. Y. Simmons, M. Pepper, D. R. Mace, W. R. Tribe, and D. A. Ritchie, Phys. Rev. B **58**, 4846 (1998).

[6] C.-K. Wang and K.-F. Berggren, Phys. Rev. B **57**, 4552 (1998).

[7] D. J. Reilly *et al.*, Phys. Rev. B **63**, 121311 (2001).

[8] K. A. Matveev, Phys. Rev. Lett. **92**, 106801 (2004).

[9] S. M. Cronenwett, H. J. Lynch, D. Goldhaber-Gordon, L. P. Kouwenhoven, C. M. Marcus, K. Hirose, N. S. Wingreen, and V. Umansky, Phys. Rev. Lett. **88**, 226805 (2002).

[10] Y. Meir, K. Hirose, and N. S. Wingreen, Phys. Rev. Lett. **89**, 196802 (2002).

[11] T. Rejec and Y. Meir, Nature (London) **442**, 900 (2006).

[12] C. Sloggett, A. I. Milstein, and O. P. Sushkov, Eur. Phys. J. B **61**, 427 (2008).

[13] F. Bauer, J. Heyder, E. Schubert, D. Borowsky, D. Taubert, B. Bruognolo, D. Schuh, W. Wegscheider, J. von Delft, and S. Ludwig, Nature (London) **501**, 73 (2013).

[14] Y. Yoon, L. Mourokh, T. Morimoto, N. Aoki, Y. Ochiai, J. L. Reno, and J. P. Bird, Phys. Rev. Lett. **99**, 136805 (2007).

[15] L. DiCarlo, Y. Zhang, D. T. McClure, D. J. Reilly, C. M. Marcus, L. N. Pfeiffer, and K. W. West, Phys. Rev. Lett. **97**, 036810 (2006).

[16] M. J. Iqbal *et al.*, Nature (London) **501**, 79 (2013).

[17] B. Brun *et al.*, Nat. Commun. **5**, 4290 (2014).

[18] L. W. Smith, A. R. Hamilton, K. J. Thomas, M. Pepper, I. Farrer, J. P. Griffiths, G. A. C. Jones, and D. A. Ritchie, Phys. Rev. Lett. **107**, 126801 (2011).

[19] A. P. Micolich, J. Phys. Condens. Matter **23**, 443201 (2011) and references therein.

[20] S. M. Grinolds, S. Hong, P. Maletinsky, L. Luan, M. D. Lukin, R. L. Walsworth, and A. Yacoby, Nat. Phys. **9**, 215 (2013).

[21] N. Kumada, K. Muraki, and Y. Hirayama, Phys. Rev. Lett. **99**, 076805 (2007).

[22] L. Tiemann, G. Gamez, N. Kumada, and K. Muraki, Science **335**, 828 (2012).

[23] M. Stern, B. A. Piot, Y. Vardi, V. Umansky, P. Plochocka, D. K. Maude, and I. Bar-Joseph, Phys. Rev. Lett. **108**, 066810 (2012).

[24] B. E. Kane, L. N. Pfeiffer, and K. W. West, Phys. Rev. B **46**, 7264 (1992).

[25] K. R. Wald, L. P. Kouwenhoven, P. L. McEuen, N. C. van der Vaart, and C. T. Foxon, Phys. Rev. Lett. **73**, 1011 (1994).

[26] D. C. Dixon, K. R. Wald, P. L. McEuen, and M. R. Melloch, Phys. Rev. B **56**, 4743 (1997).

[27] S. Kronmuller, W. Dietsche, K. v. Klitzing, G. Denninger, W. Wegscheider, and M. Bichler, Phys. Rev. Lett. **82**, 4070 (1999).

[28] M. Kawamura, H. Takahashi, K. Sugihara, S. Masubuchi, K. Hamaya, and T. Machida, Appl. Phys. Lett. **90**, 022102 (2007).

[29] W. Desrat D. K. Maude, M. Potemski, J. C. Portal, Z. R. Wasilewski, and G. Hill, Phys. Rev. Lett. **88**, 256807 (2002).

[30] C. P. Slichter, *Principles of Nuclear Magnetism* (Oxford University Press, New York, 1984).

[31] Y. Ren, W. Yu, S. M. Frolov, J. A. Folk, and W. Wegscheider, Phys. Rev. B **81**, 125330 (2010).

[32] N. R. Cooper and V. Tripathi, Phys. Rev. B **77**, 245324 (2008).

[33] P. Stano and D. Loss, Phys. Rev. B **90**, 195312 (2014).

[34] M. Kawamura, M. Ono, Y. Hashimoto, S. Katsumoto, K. Hamaya, and T. Machida, Phys. Rev. B **79**, 193304 (2009).

[35] M. Kawamura, D. Gottwald, K. Ono, T. Machida, and K. Kono, Phys. Rev. B **87**, 081303 (2013).

[36] See Supplemental Material at http://link.aps.org/supplemental/10.1103/PhysRevLett.115.036601, which includes Refs. [37–40], for details on electric quadrupole splitting, stability of an external magnetic field, determination of the hyperfine coupling constant α_{As}, an alternative fitting analysis, and the tight-binding model calculation.

[37] K. A. Dumas, J. F. Soest, A. Sher, and E. M. Swiggard, Phys. Rev. B **20**, 4406 (1979).

[38] D. Paget, G. Lampel, B. Sapoval, and V. I. Safarov, Phys. Rev. B **15**, 5780 (1977).

[39] J. Schliemann, A. Khaetskii, and D. Loss, J. Phys. Condens. Matter **15**, R1809 (2003).

[40] T. Ando, Phys. Rev. B **44**, 8017 (1991).

[41] The small ac voltage V_{ac} (20 μV, 118 Hz) was not turned off during this period of 22 s. Although the small V_{ac} might induce DNSP, its amplitude is much smaller than that induced by $V_{\mathrm{sd}} = -300$ μV at the first step.

[42] P. Khandelwal, N. N. Kuzma, S. E. Barrett, L. N. Pfeiffer, and K. W. West, Phys. Rev. Lett. **81**, 673 (1998).

[43] The parameter $w_z = (18 \pm 3)$ nm is typical for the interface of GaAs/AlGaAs [44]. The parameter $w_y = (65 \pm 5)$ nm, which is related to the intersubband energy, is determined from the gate-voltage width of the first conductance plateau.

[44] T. Ando, J. Phys. Soc. Jpn. **51**, 3900 (1982).

[45] S. Datta, *Quantum Transport: Atom to Transistor* (Cambridge University Press, Cambridge, England, 2005).